NASA Technical Memorandum 81892



# Flight Evaluation of the Effect of Winglets on Performance and Handling Qualities of a Single-Engine General Aviation Airplane

Bruce J. Holmes, Cornelis P. van Dam,
Philip W. Brown, and Perry L. Deal

DECEMBER 1980



NASA

NASA Technical Memorandum 81892

# Flight Evaluation of the Effect of Winglets on Performance and Handling Qualities of a Single-Engine General Aviation Airplane

Bruce J. Holmes
*Langley Research Center*
*Hampton, Virginia*

Cornelis P. van Dam
*University of Kansas*
*Lawrence, Kansas*

Philip W. Brown and Perry L. Deal
*Langley Research Center*
*Hampton, Virginia*

National Aeronautics
and Space Administration

**Scientific and Technical
Information Branch**

1980

## SUMMARY

A flight evaluation was conducted to determine the effects of winglets on the performance and handling qualities of a light, single-engine general aviation airplane. The performance measurements were made with a pace airplane to provide calibrated airspeeds; uncalibrated panel instruments in the test airplane were used to provide additional quantitative peformance data. These tests were conducted with winglets on and off during the same day to measure relative performance effects. Handling qualities were evaluated by means of pilot comments.

Performance measurements showed winglets increased cruise speed 8 knots (5.6 percent) at a density altitude of 3962 m (13 000 ft) and a setting of 51 percent maximum continuous power. Maximum speed at this altitude was virtually unchanged. Rate of climb increased approximately 6 percent, or 0.25 m/sec (50 ft/min), at 1524 m (5000 ft). Stall speed was virtually unchanged, and handling qualities were favorably affected.

## INTRODUCTION

The current rising cost of fuel has led to increased research on methods for increasing fuel efficiency for all categories of aircraft. Recent experiments (refs. 1 to 3) have demonstrated that for transport and business-jet aircraft, winglets can increase aerodynamic/structural efficiency. Experiments have also shown that winglets added onto an existing wing can improve climb performance for low-speed STOL transport aircraft with small empty-weight penalties (ref. 4). The present tests were conducted to investigate the effects winglets can have on the performance and handling qualities of a general aviation airplane with somewhat low wing loading.

Aerodynamic analyses have indicated that an increase in twist and taper and a decrease in wing loading can combine to unload the wing tip sufficiently to negate winglet performance benefits at cruise lift coefficients. However, many general-aviation-airplane wings are designed to carry sufficient aerodynamic loading near the tip to allow successful use of winglets for drag reduction. The flight evaluation reported herein resulted in data which support predictions of the aerodynamic benefits of winglets on a representative general-aviation-airplane wing.

Based on the present investigation, winglets can have a beneficial effect on airplane handling qualities at the stall, which has not been previously reported. Experiments reported in the literature have shown that the installation of winglets on one airplane configuration degraded high-angle-of-attack handling qualities (ref. 4). Cases have also been reported in which winglets did not alter the high-angle-of-attack handling qualities (ref. 3). Apparently these effects are sensitive to particular combinations of winglets and wing geometries. This paper presents pilot comments on handling qualities near the stall

along with a discussion of stability and control parameters which could have produced the beneficial effects that were observed for the configuration tested.

## SYMBOLS

Except for airspeed, which is given in knots, data are presented in the International System of Units (SI) with the equivalent values given parenthetically in the U.S. Customary Units. Measurements and calculations were made in U.S. Customary Units. Factors relating the two systems of units are given in reference 5.

| | |
|---|---|
| $A$ | geometric aspect ratio, $b^2/S$ |
| $A_e$ | effective airplane aspect ratio, $A\left(1 + 1.1\,\frac{S_e}{S}\right)$ |
| $b$ | wing span, m (ft) |
| $C_D$ | trimmed, power-on drag coefficient, $P_T/qVS$ |
| $C_{D,o}$ | airplane zero-lift drag coefficient |
| $C_L$ | trimmed, power-on lift coefficient, $W/qS$ |
| $C_L'$ | trimmed, power-on lift coefficient based on indicated airspeed and standard sea-level density, $W/(1/2\ \rho_o V_i^2 S)$ |
| $C_{L,m}$ | airplane lift coefficient for maximum lift-drag ratio |
| $C_l$ | rolling-moment coefficient, Rolling moment/qSb |
| $C_{l\delta_a}$ | rolling moment due to aileron deflection, $\partial C_l/\partial\delta_a$, $deg^{-1}$ |
| $C_n$ | yawing-moment coefficient, Yawing moment/qSB |
| $C_{n\delta_a}$ | yawing moment due to aileron deflection, $\partial C_n/\partial\delta_a$, $deg^{-1}$ |
| $C_{n\beta}$ | yawing moment due to sideslip, $\partial C_n/\partial\beta$, $deg^{-1}$ |
| $C_Y$ | side-force coefficient, Side force/qS |
| $C_{Y\beta}$ | side force due to sideslip, $\partial C_Y/\partial\beta$, $deg^{-1}$ |
| $D$ | airplane trimmed, power-on drag, N (lb) |
| $e$ | Oswald efficiency factor, $1/\pi A\left[d\left(C_L^2\right)/d(C_D)\right]$ |
| $L$ | airplane trimmed, power-on lift, N (lb) |
| $M$ | Mach number |

| | |
|---|---|
| $P_T$ | thrust power, kW (hp) |
| $p$ | static air pressure, $N/m^2$ ($lb/ft^2$) |
| $q$ | dynamic pressure, $1/2\ \rho V^2$, $N/m^2$ ($lb/ft^2$) |
| $S$ | wing planform area, $m^2$ ($ft^2$) |
| $S_e$ | sum of end-plate areas projected in vertical plane, $m^2$ ($ft^2$) |
| $T$ | static air temperature, K ($^oR$) |
| $V$ | true airspeed, knots |
| $V_c$ | calibrated airspeed, knots |
| $V_i$ | indicated airspeed including position error and instrument error, knots |
| $V_m$ | true airspeed for maximum lift-drag ratio, knots |
| $V_s$ | stall speed in given configuration, knots |
| $W$ | airplane weight, N (lb) |
| $W_i$ | airplane weight at test point, N (lb) |
| $\beta$ | sideslip angle, deg |
| $\Delta V_c$ | airspeed position error, $V_i - V_c$, knots |
| $\delta_a$ | aileron deflection, deg |
| $\eta_p$ | propeller efficiency |
| $\rho$ | air density, $kg/m^3$ ($slugs/ft^3$) |

Subscripts:

| | |
|---|---|
| max | maximum |
| o | standard sea-level condition |
| std | standard condition or condition at selected altitude |

## DESCRIPTION OF AIRPLANE AND TESTING

The flight evaluation was conducted with a light, single-engine six-passenger, retractable-gear general aviation airplane. (See figs. 1 to 4 and table I.) The baseline airplane (without winglets) is described in reference 6. Details of the airplane design are listed in table I. The winglets were built

of fiberglass skins with full-depth foam core material. The weight of the winglets was 133 N (30 lb), and the weight of the standard wing tips was 44 N (10 lb). Thus, the airplane empty-weight increase due to the winglet installation was 89 N (20 lb).

The standard uncalibrated panel instruments in the test airplane were used to record performance parameters. Indicated airspeed was calibrated for position error with winglets on and off by the pace-airplane technique (ref. 7). The effect power had on position error was also measured.

All performance data were measured with winglets on and off during the same day. During these flight tests, a neutral temperature gradient existed between 1524 m (5000 ft) and 3048 m (10 000 ft) pressure altitudes. Such conditions provided a very stable air mass with minimal vertical air motion, generally considered optimal for conducting performance flight tests.

Level-flight speed-power measurements were made with the basic airplane and with the airplane equipped with winglets from top speed to stall at a pressure altitude of 1524 m (5000 ft). Sawtooth climb data were gathered at pressure altitudes of 1524 m and 3658 m (12 000 ft) for both configurations. At 3962 m (13 000 ft) pressure altitude, level-flight speed-power data were taken at 51 percent of maximum continuous power and at full-throttle settings (62.5 percent of maximum continuous power).

Handling qualities of the basic airplane and the winglet-equipped airplane were evaluated in cruise and power-approach (landing gear and flaps down, $V_i$ = 80 knots) configurations. Maximum-deflection aileron rolls were conducted to evaluate the effect of winglets on roll performance. Correlations between control forces, control deflections, and resulting airplane attitude changes were evaluated using pilot comments. The effects of winglets on stall behavior were evaluated for wings level and for accelerated stalls, with and without sideslip.

Airplane handling qualities and performance at high (prestall) angles of attack were further evaluated by flying a task requiring lateral and longitudinal control of the airplane. The task began with the airplane trimmed with power for level flight at $1.3V_S$ in a climb configuration (flaps and gear up). Next the throttle was idled, the controls were held fixed for 3 sec (simulating delayed pilot response to an engine failure), and a 180° heading reversal was flown while attempting to minimize altitude loss. Following an engine failure after take-off, such a maneuver might be attempted by a pilot in an effort to return to the runway. Approximately five repetitions of the task were conducted by the same pilot on the same day for winglets on and off.

During the evaluations of stalls and high-angle-of-attack handling qualities, video tape recordings of tuft patterns on the right wing (and winglet) were made with winglets on and off.

## DATA REDUCTION

During steady level flight, readings were taken from test-airplane and pace-airplane panel instruments. Calibrated airspeed was obtained from indicated airspeed from the pace airplane and the calibration charts of reference 7; thus, $V_C = V_i - \Delta V_C$. True airspeed was calculated from calibrated airspeed, ambient temperature, and pressure (calculated from indicated pressure altitude) in the following manner:

$$V = V_C \sqrt{\frac{p_o T}{p T_o}} \qquad (M \leq 0.2) \qquad (1)$$

For the test airplane, engine brake power was determined from engine manifold pressure, revolutions per minute, pressure altitude, ambient temperature, and the power chart supplied by the engine manufacturer. Thrust power was computed from brake power and the manufacturer's propeller performance chart; thus, $P_T = \eta_p \times$ Brake power.

Drag coefficient was determined as follows (for SI units):

$$C_D = \frac{P_T}{\frac{1}{2} \rho V^3 S} \qquad (2)$$

where $\rho$ was determined from static temperature and pressure calculated from indicated pressure altitude. Airplane weight was determined for each test point by plotting the approximate fuel consumed against time and from the initial and final weight of the airplane. The lift coefficient was calculated in the following manner:

$$C_L = \frac{W}{\frac{1}{2} \rho V^2 S} \qquad (3)$$

In order to plot thrust power as a function of airspeed for the airplane at a gross weight, the flight test data were corrected to standard density altitude and weight as follows:

$$P_{T,std} = P_T\left(\frac{\rho}{\rho_{std}}\right)^{0.5}\left(\frac{W_{std}}{W_i}\right)^{1.5} \tag{4}$$

$$V_{std} = V\left(\frac{\rho}{\rho_{std}}\right)^{0.5}\left(\frac{W_{std}}{W_i}\right)^{0.5} \tag{5}$$

The sawtooth climb data were corrected to standard density altitude and weight at a point midway in each climb segment.

The specific range at the airplane gross weight was determined from the airplane drag polar and the fuel-flow-versus-brake-power chart supplied by the engine manufacturer. The analysis of performance data may be simplified by assuming the data fit a parabolic drag polar, symmetric about zero lift. Then maximum lift-to-drag ratio is given by

$$(L/D)_{max} = \frac{1}{2}\sqrt{\frac{\pi Ae}{C_{D,o}}} \tag{6}$$

and the lift coefficient for maximum lift-to-drag ratio is given by

$$C_{L,m} = \sqrt{\pi Ae C_{D,o}} \tag{7}$$

## DISCUSSION OF RESULTS

### Airspeed Calibration

In figure 5, the airspeed calibration data are shown for the airplane in the winglet-on and winglet-off configurations. The data indicate that the installation of winglets leaves the airspeed calibration virtually unaffected. This is expected since the static ports on the fuselage are far removed from the winglets and their effect on circulation patterns. The airspeed calibration from reference 6 is also shown in figure 5. The curve shows the same trends as the measured airspeed-position error curve. Power effects on the airspeed calibration appear to be negligible for the climb, cruise, and idle power conditions tested.

### Performance

The drag polars of the airplane with and without winglets are shown in figure 6. The drag coefficients include the increase in drag due to propeller-slipstream effects. Both lift and drag coefficients contain thrust contributions in all data presented herein; that is, all data are presented at power for level-flight conditions. The installation of winglets alters the zero-lift drag

as well as the lift-induced drag. The zero-lift drag increases slightly due to the increase in wetted area. The lift-induced drag decreases as indicated by the increase in the Oswald efficiency factor. At the lower lift coefficients, the increase in zero-lift drag offsets the decrease in lift-induced drag and this will result in a slightly higher drag. The crossover for the test airplane, however, occurs at a relatively low lift coefficient ($C_L = 0.266$) as shown in figure 6. The numerically faired drag-polar equations listed in figure 6 are valid for $C_L > 0.2$.

In figure 7, the effect of winglets on the Oswald efficiency factor is shown. The installation of winglets causes the Oswald efficiency factor to increase by 13 percent. In reference 8, the following empirically derived expression is presented to approximate the effect of wing end-plates on induced drag:

$$A_e = A\left(1 + 1.1\,\frac{S_e}{S}\right) \tag{8}$$

The airplane, shown in figures 1 to 4, had a ratio of end-plate areas to planform area $S_e/S$ of 0.056. By using the end-plate theory in equation (8), the effective aspect ratio could be expected to increase from $A = 6.20$ to $A = 6.58$ (6 percent). The theoretical potential-flow method of reference 2 predicts an increase in efficiency factor due to winglet installation near the experimentally obtained value of 13 percent.

Speed-power data for the basic airplane and for the winglet-equipped airplane at sea level, 1524 m (5000 ft), and 3962 m (13 000 ft) density altitudes are presented in figures 8 to 10. The power-available curves are obtained from propeller and engine manufacturer information. The power-required curves are obtained from the numerically faired drag polars of figure 6. Figures 8 to 10 indicated that at any altitude and for any power setting below 65 percent, the steady, level-flight power required is less for the winglets-on configuration (i.e., at $C_L > 0.266$). These altitudes and power settings largely comprise the most practical cruise conditions for this airplane. As seen in figure 10, cruise speed at 3962 m density altitude and 51 percent power setting is increased by about 8 knots. Maximum speed at this altitude is virtually unchanged. However, at lower altitudes the maximum speed is reduced.

The drag polars in figure 6 and the thrust-power plots in figures 8 to 10 indicate that the winglets improve the climb performance of the airplane significantly. The climb is performed at a lift coefficient of about 0.7. In figure 11, the rate of climb is shown as a function of density altitude. The increment in rate of climb due to winglets increases with altitude. The winglets improve climb performance by about 0.25 m/sec (50 ft/min) at low altitude (1524 m (5000 ft)), and the increment is about 0.80 m/sec (157 ft/min) at high altitude (3658 m (12 000 ft)). This effect is expected since as altitude increases, lift coefficient for maximum rate of climb increases. At these higher coefficients, the benefit of winglet installation increases by reducing the induced-drag penalty in climb.

Figure 6 indicates that the range factor $(L/D)_{max} = \frac{1}{2}\sqrt{\frac{\pi Ae}{C_{D,o}}}$ increases due to the installation of winglets. The maximum lift-to-drag ratio $(L/D)_{max}$ increases by 11 percent. However, due to the increases in zero-lift drag and Oswald efficiency factor, the lift coefficient for $(L/D)_{max}$ (i.e., $C_{L,m} = \sqrt{\pi Ae C_{D,o}}$) also increases from $C_{L,m} = 0.51$ for the basic airplane to $C_{L,m} = 0.55$ for the airplane with winglets.

Presented in figure 12 is a plot which demonstrates the effect of winglets on the airplane specific range. This plot shows that winglets decrease the specific range during fast cruise at low altitudes, which corresponds with a low lift coefficient ($C_L < 0.266$). In all other cases, however, installation of winglets improves the fuel efficiency of the airplane. The increase in $C_{L,m}$ produces a decrease in airplane velocity for maximum lift-to-drag ratio $V_m$ from 116 knots to 111 knots at 1524 m (5000 ft) density altitude. Alternatively, increased $C_{L,m}$ requires a higher altitude for maximum fuel economy at a given speed. This latter effect is reflected in figure 12 in which, at an airspeed of 120 knots, the altitude for peak fuel efficiency increases from 2207 m (7240 ft) for winglets off to 3059 m (10 035 ft) for winglets on. In spite of the slightly lower speed for cruise at $(L/D)_{max}$ and the higher altitude required for maximum fuel economy at a given speed, the absolute benefit of winglets on fuel economy is significant for all conditions except high speed (160 knots) at low altitudes. (See fig. 12.)

Although winglets offer advantages as a retrofit application to existing aircraft, the potential fuel-efficiency gains which might be realized may be limited by the existing wing structure and aerodynamic characteristics. If an airplane was designed with a combined wing-winglet lifting system instead of as a retrofit application, more effective application of winglets might result. Reference 9 contains one such design study, illustrating the structural (empty weight) benefits of an optimized wing-winglet design over a conventional wing design. In addition to providing a weight savings (as noted in ref. 9), the wing-winglet combination can be optimized to a higher wing loading for a given value of induced drag. If the design is not constrained by maximum allowable stall speed, wing loading can be increased to permit a closer match between cruise speed and $V_m$ as $V_m$ increases with wing loading. Alternative methods of exploiting the winglet benefits include increasing the cruise speed (if the design is not constrained by flutter or compressibility problems) or decreasing the design cruise altitude (at increased $W/S$ and constant $V_m$). These possible design alternatives can be illustrated by observing the effects of changing wing loading, airspeed, or altitude (density) in the following expression for flight at $(L/D)_{max}$:

$$\frac{W}{S} = C_{L,m}\,\frac{1}{2}\,\rho V_m^2 \tag{9}$$

Remember that $C_{L,m}$ is fixed by the constant induced drag requirement.

In general, the best method of utilizing an optimized wing-winglet lifting system will depend strongly on the particular airplane mission. The wing-winglet optimization for medium-speed, general aviation aircraft will differ from that for transport aircraft since flutter, compressibility, and drag rise may not penalize winglet installation.

## Handling Qualities

The winglets on the test airplane had no noticeable effect on longitudinal stability and control (cruise and approach). The most interesting stability and control effects were in the lateral directional modes as would be expected. The dihedral effect was positive (negative rolling moment caused by positive sideslip) for the basic airplane and the winglet-equipped airplane. However, the winglet-equipped airplane had an increased roll rate for a given rudder input, indicating increased dihedral effect (assuming the winglets had no effect on $C_{n_\beta}$). Lateral control using rudder only was improved with the installation of the winglets. The side force produced (determined by bank angle) in maximum-rudder, steady-heading sideslips $C_{Y_\beta}$ with the winglet-equipped airplane was approximately 50 percent greater than the side force produced with the basic airplane.

During the adverse-yaw tests, the airplane with winglets produced an initial slight adverse yaw (moderate amount of aileron and free rudder) which was easily coordinated with a small amount of rudder if desired. The amount of adverse yaw generated with a moderate amount of aileron deflection to roll to a bank angle of $30^\circ$ was so small that rudder coordination was not considered necessary. The basic airplane displayed a slightly different behavior. Initially, as the roll input was made the yaw went slightly proverse, oscillated to slightly adverse, then to zero as the desired bank angle was reached. The yaw generated with aileron input $C_{n_{\delta_a}}$ was very small and oscillatory; rudder coordination during this oscillation was neither possible nor considered necessary. In general, differences in $C_{n_{\delta_a}}$ between winglets-on and winglets-off configurations had an insignificant effect on handling qualities during cruise and approach tasks. The service aileron-rudder-interconnect in the airplane favorably influenced any roll-yaw coupling in the airplane.

Heading control during roll-out of a turn was a little smoother and easier with the winglets installed. The basic airplane displayed heading-overshoot tendencies, whereas the airplane with winglets did not show this behavior.

Neither the basic airplane nor the winglet-equipped airplane showed objectionable control-force, control-displacement, side-force, and/or pitching-moment nonlinearities while traversing the range of sideslip angles during steady-heading sideslips.

Stalling the forward winglet at large angles of sideslip did not change the balance of forces and moments noticeably. The stalled winglet did not induce a separated flow region on the wing upper surface as happened with other winglet-

equipped aircraft (e.g., the airplane of ref. 4). During straight-ahead stalls, the winglets stalled before the wing.

The roll rate due to maximum aileron deflection appeared to be slightly greater for the winglet-equipped airplane. This might be explained by the effect of winglets on the span loading. Winglets increase the local span loading near the wing tips, thereby augmenting aileron effectiveness $C_{l_{\delta_a}}$. In addition, the downward deflection of an aileron may induce an increased flow angle of attack on the winglet, thus increasing rolling moments generated by a given aileron deflection. Some effect of winglets on roll damping might be expected due to endplate effect; however, no effect was observable during the present tests.

The installation of the winglets did not noticeably change the spiral mode and Dutch-roll mode for the conditions tested. These effects might be expected since winglets installed on unswept wings tend to have an insignificant effect on $C_{n_\beta}$.

The stall speeds for the airplane with winglets were slightly lower than those of the basic airplane. In the case of no-sideslip stalls, both the basic airplane and the airplane with winglets stalled with mild pitch breaks. However, at the stall, the basic airplane displayed a tendency to roll-off or drop a wing. The winglet-equipped airplane displayed much less of this roll-off tendency. The winglets appeared to prevent the wing tips from stalling early, reducing the tendency for roll-off. During moderate sideslips (one-half-ball deflection) with wings level and slow deceleration to the stall, the basic airplane rolled-off rapidly toward the trailing wing. With winglets on, lateral control could be maintained with ailerons throughout stalls with moderate sideslip.

During slow flight, both the basic airplane and the airplane with winglets were maneuverable and relatively undemanding in coordination of stick and rudder pedals.

During the simulated engine-out heading reversals, the pilot made turns just below the stalling angle of attack with the stall-warning horn on and some light airframe buffet. Following the heading-reversal maneuver, the basic airplane had lost an average of 91 m (300 ft) altitude whereas the airplane with winglets lost an average of 76 m (250 ft) during the identical maneuver. These altitude losses were readily repeatable.

Research pilots commented that in general the winglets had a beneficial effect on the handling qualities of the airplane at cruise, landing approach, and stall.

## CONCLUDING REMARKS

A flight evaluation was performed to determine the effects of winglets on the performance and handling qualities of a light, single-engine, six-passenger general aviation airplane. The performance measurements were made with a pace airplane to provide calibrated airspeeds. Uncalibrated panel instruments in

the test airplane were used to provide additional quantitative performance data. The flight tests were conducted with winglets on and winglets off. Handling qualities were evaluated by means of pilot comments. The results indicate the following:

1. Adding the winglets increased the Oswald efficiency factor by 13 percent; the increase in maximum lift-to-drag ratio was 11 percent.

2. Winglets left the maximum speed at 3962 m (13 000 ft) density altitude virtually unchanged. At lower altitudes, however, the maximum speed was reduced. Cruise speed increased 8 knots (5.6 percent) at 3962 m and 51 percent maximum continuous power.

3. An improvement in climb performance was obtained due to the installation of winglets. Rate of climb increased approximately 0.25 m/sec (50 ft/min), or 6 percent, at 1524 m (5000 ft) and by a greater amount at higher altitude.

4. Winglets increased the fuel efficiency of the airplane for $C_L > 0.266$.

5. Handling qualities were favorably affected by the installation of winglets.

Langley Research Center
National Aeronautics and Space Administration
Hampton, VA 23665
October 29, 1980

## REFERENCES


1. Whitcomb, Richard T.: A Design Approach and Selected Wind-Tunnel Results at High Subsonic Speeds for Wing-Tip Mounted Winglets. NASA TN D-8260, 1976.

2. Heyson, Harry H.; Riebe, Gregory D.; and Fulton, Cynthia L.: Theoretical Parametric Study of the Relative Advantages of Winglets and Wing-Tip Extensions. NASA TP-1020, 1977.

3. Reynolds, P. T.: The Learjet Longhorn Series - The First Jets With Winglets. Preprint 790581, Soc. Automot. Eng., Apr. 1979.

4. Eliraz, Y.; and Ilan, D.: Performance of the ARAVA Aircraft With Wing-Tip Winglets. Israel J. Technol., vol. 15, nos. 1-2, 1977, pp. 35-43.

5. Standard for Metric Practice. E 380-79, American Soc. Testing & Mater., c.1980.

6. Pilot's Operating Handbook and FAA Approved Airplane Flight Manual for the Beechcraft Bonanza A36 (E-927 and After). P/N 36-590002-17, Commercial Product Support, Beech Aircraft Corp., Oct. 1976. (Rev. Sept. 1979.)

7. Holmes, Bruce J.: Low-Speed Airspeed Calibration Data for a Single-Engine Research-Support Airplane. NASA TM-81832, 1980.

8. Hoerner, Sighard F.: Fluid-Dynamic Drag. Hoerner Fluid Dynamics (Brick Town, N.J.), c.1965.

9. Shollenberger, C. A.: Application of an Optimized Wing-Winglet Configuration to an Advanced Commercial Transport. NASA CR-159156, 1979.

TABLE I.- GEOMETRY OF BASIC AIRPLANE AND WINGLETS

| | |
|---|---|
| Gross weight, N (lb) | 16 013 (3600) |
| **Wing:** | |
| Area, $m^2$ ($ft^2$) | 16.8 (181.0) |
| Wing loading, $N/m^2$ ($lb/ft^2$) | 952 (19.9) |
| Span without winglets, m (ft) | 10.2 (33.5) |
| Span with winglets (geometric), m (ft) | 10.68 (35.05) |
| Aspect ratio without winglets (geometric) | 6.20 |
| Taper ratio | 0.50 |
| Airfoil section: | |
| Root | NACA 23016.5 (modified) |
| Tip | NACA 23012 (modified) |
| Root chord, m (in.) | 2.13 (84.0) |
| Tip chord, m (in.) | 1.07 (42.0) |
| Twist (washout), deg | 3.0 |
| Dihedral, deg | 6.0 |
| Incidence at root, deg | 4.0 |
| Sweep at half chord, deg | 0 |
| **Winglet:** | |
| Length, m (in.) | 0.91 (36.0) |
| Root chord, m (in.) | 0.71 (28.0) |
| Tip chord, m (in.) | 0.36 (14.0) |
| Area (projected vertically), $m^2$ ($ft^2$) | 0.47 (5.07) |
| Aspect ratio (based on vertically projected geometry) | 1.65 |
| Taper ratio | 0.5 |
| Sweep at quarter chord, deg | 30.0 |
| Twist, deg | 0 |
| Incidence at root, deg | -2.0 |
| Cant angle, deg | 15.0 |
| Airfoil section | LS(1)-0413 |
| Thickness ratio, percent of chord | 13.0 |
| **Powerplant:** | |
| Manufacturer[1] | Teledyne Continental Motors |
| Model | IO-520-BA |
| Take-off and maximum continuous power, kW (hp) | 213 (285) |
| Revolutions per minute | 2700 |
| **Propeller (constant speed):** | |
| Manufacturer | McCauley Acc. Div. Cessna Aircraft Co. |
| Number of blades | 3 |
| Hub type | 3A32C76 |
| Blade type | 82NB-2 |

[1]Use of trade names or names of manufacturers in this report does not constitute an official endorsement of such products or manufacturers, either expressed or implied, by the National Aeronautics and Space Administration.

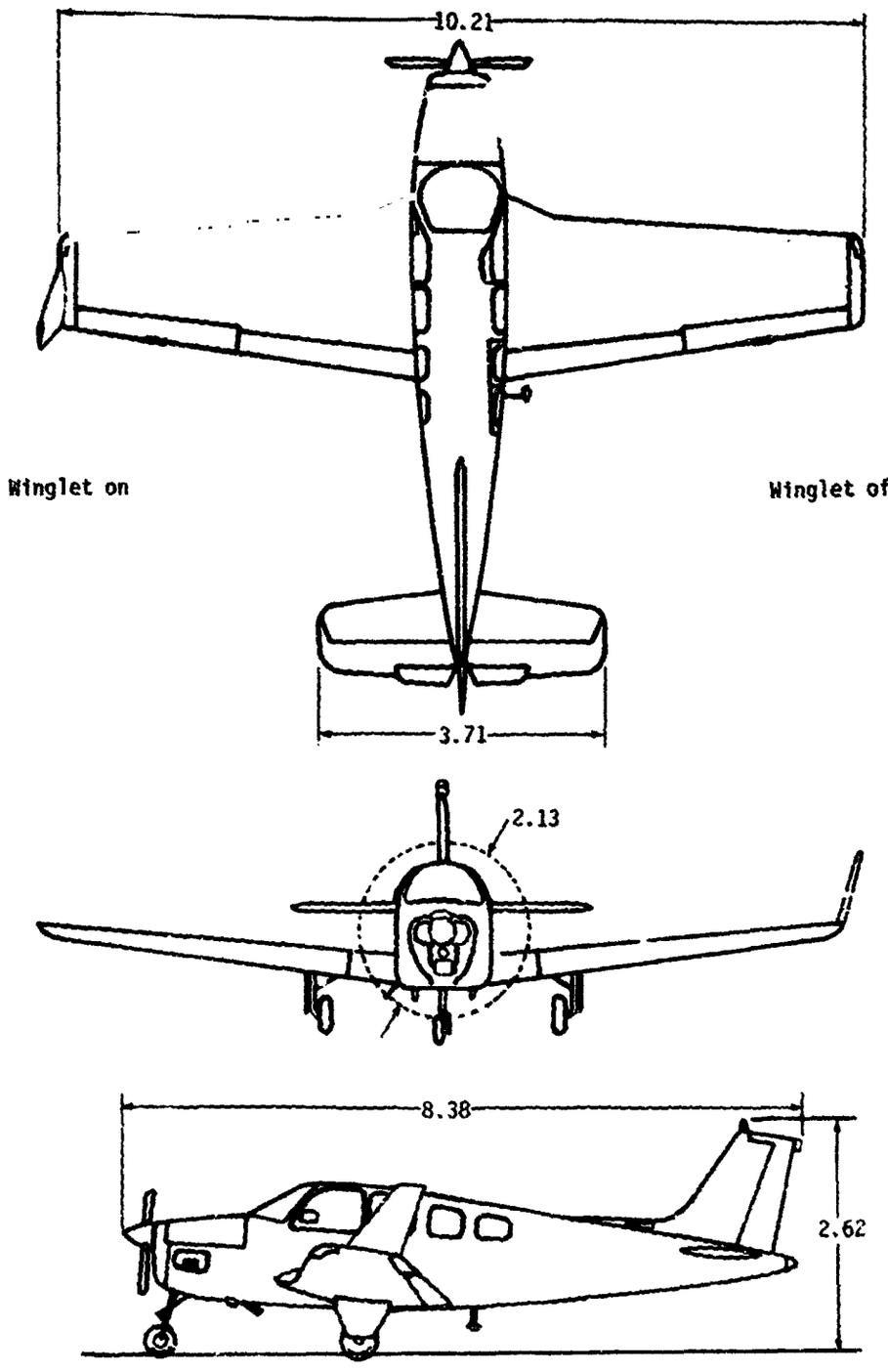


(a) Three views of airplane with and without winglets.

Figure 1.- General layout of test airplane. Dimensions are in meters unless otherwise noted.

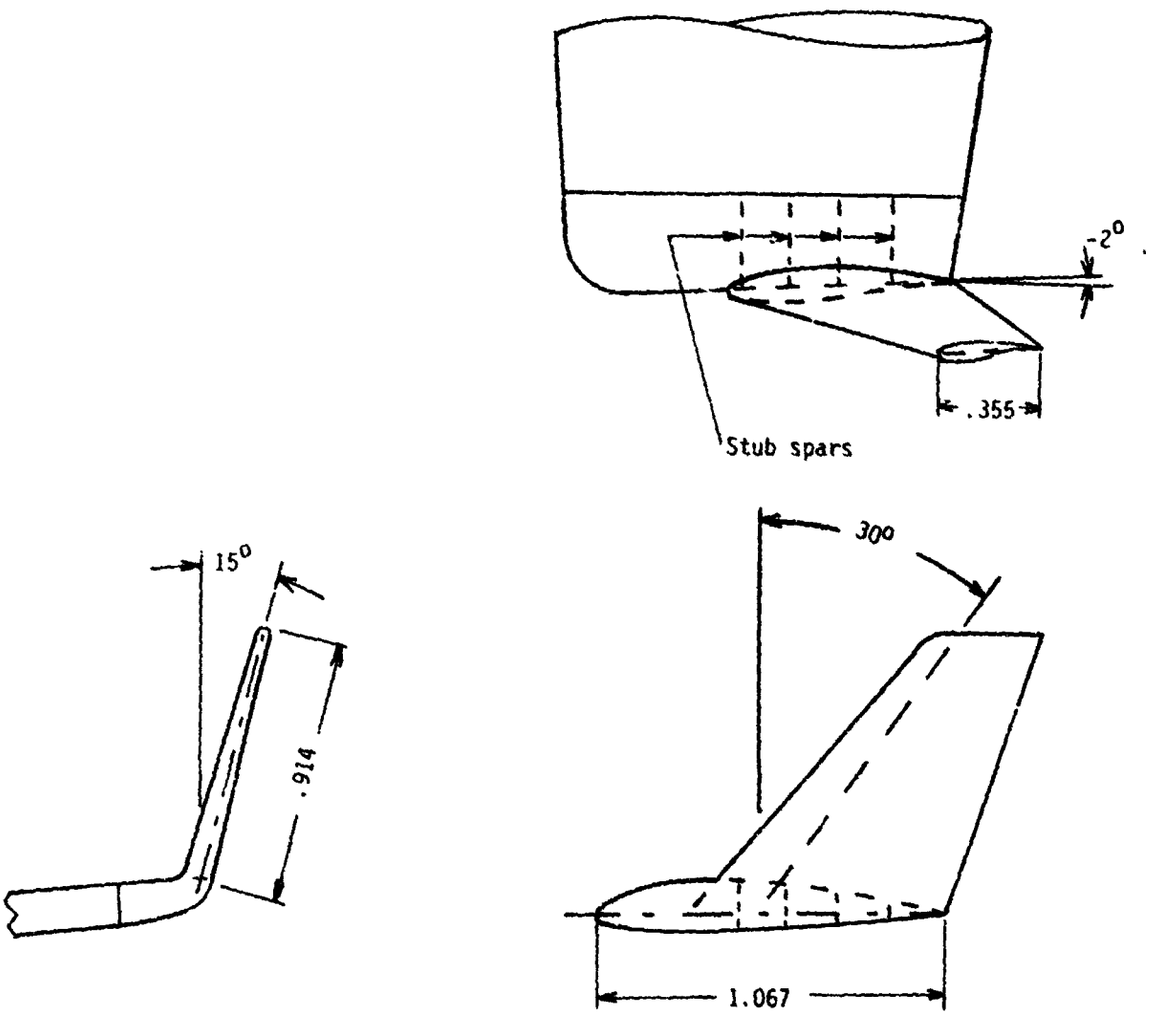


(b) Winglet detail.

Figure 1.- Concluded.

L-80-200

Figure 2.- Test airplane with winglets.

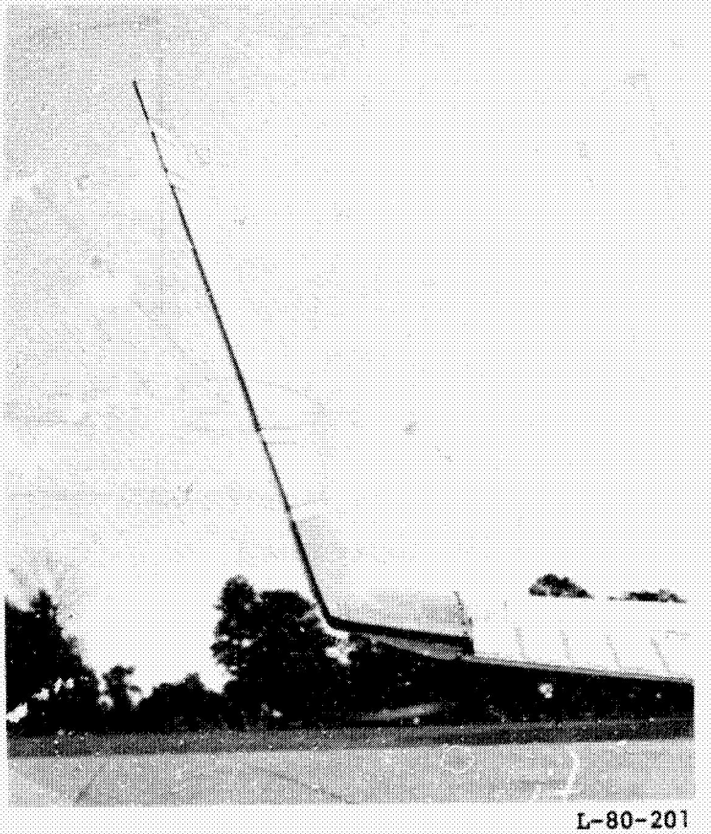

L-80-201

Figure 3.- Rear view of left winglet.

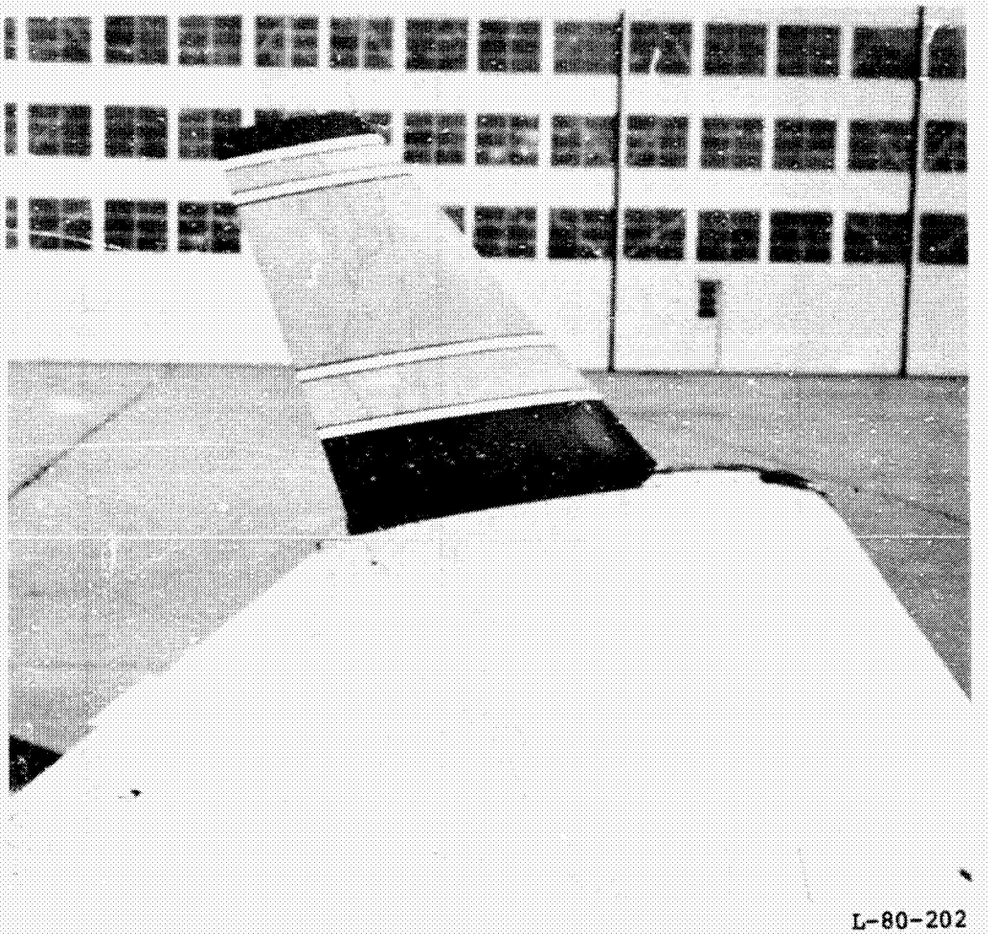

L-80-202

Figure 4.- Inboard side view of winglet.

$$C_L' = \frac{W_i}{1/2\ \rho_o\ V_i^2\ S}$$

$$V_c = V_i - \Delta V_c$$

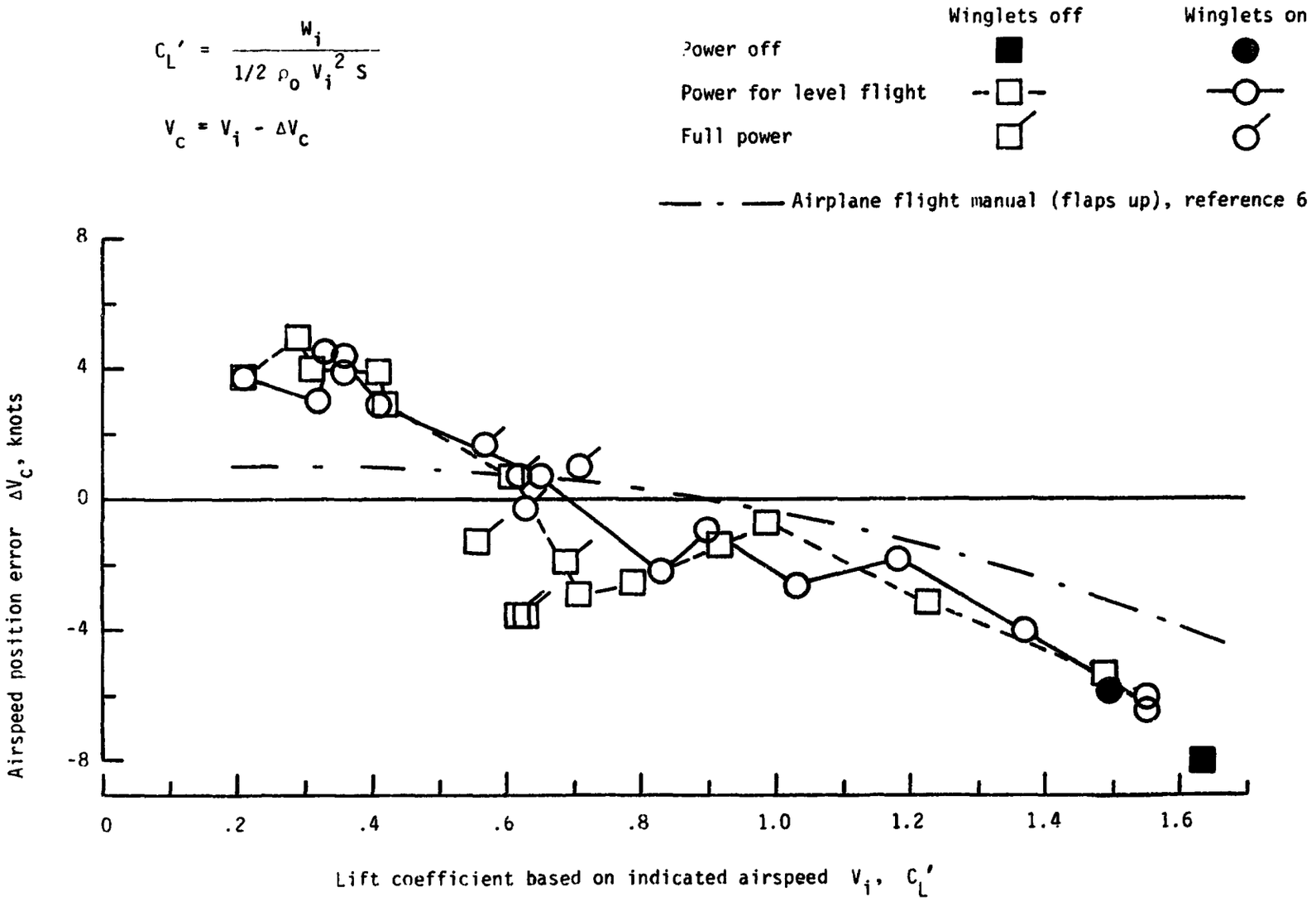


Figure 5.- Airspeed calibration from pace-airplane method.

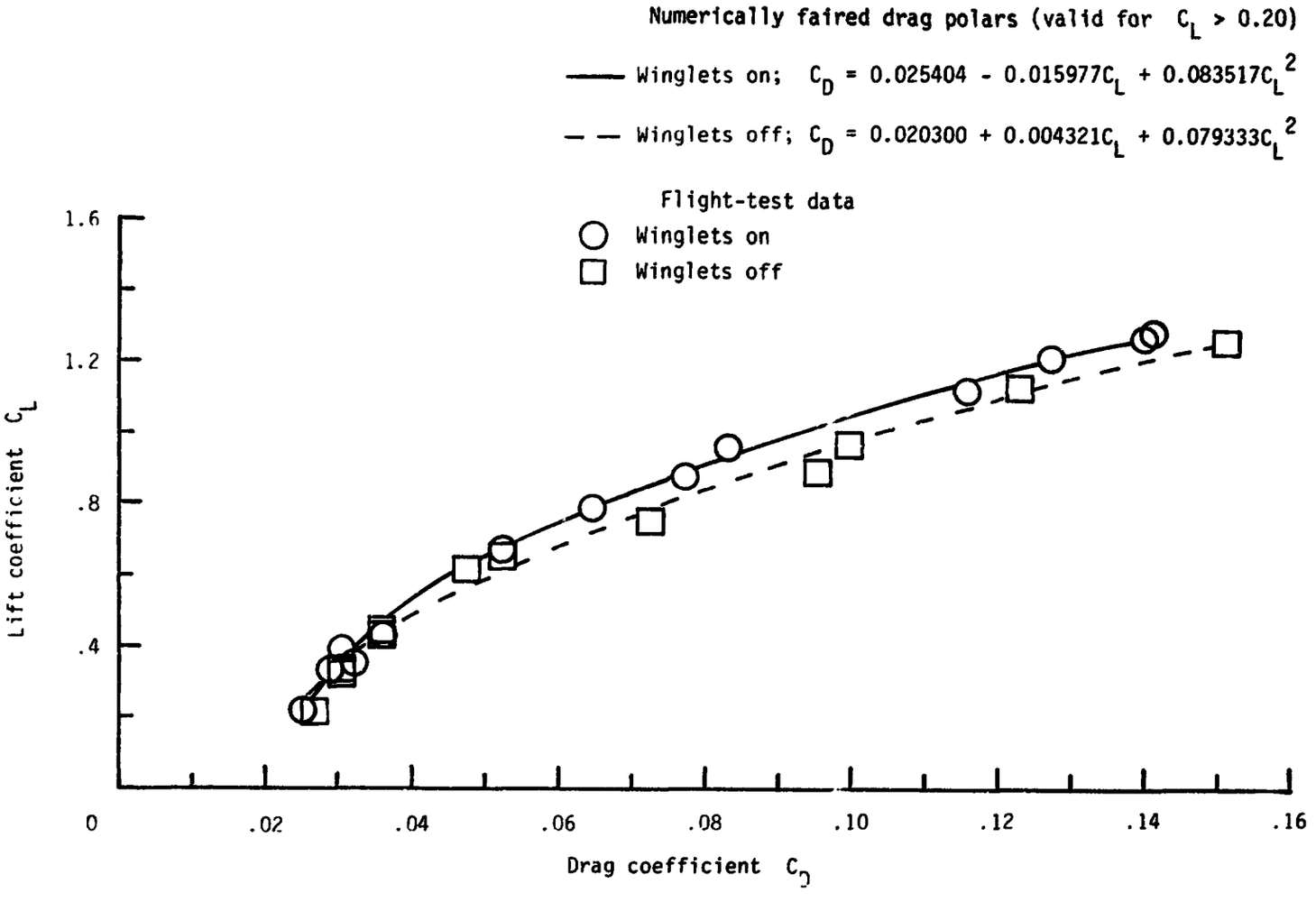


**Figure 6.- Effect of winglets on airplane drag.**

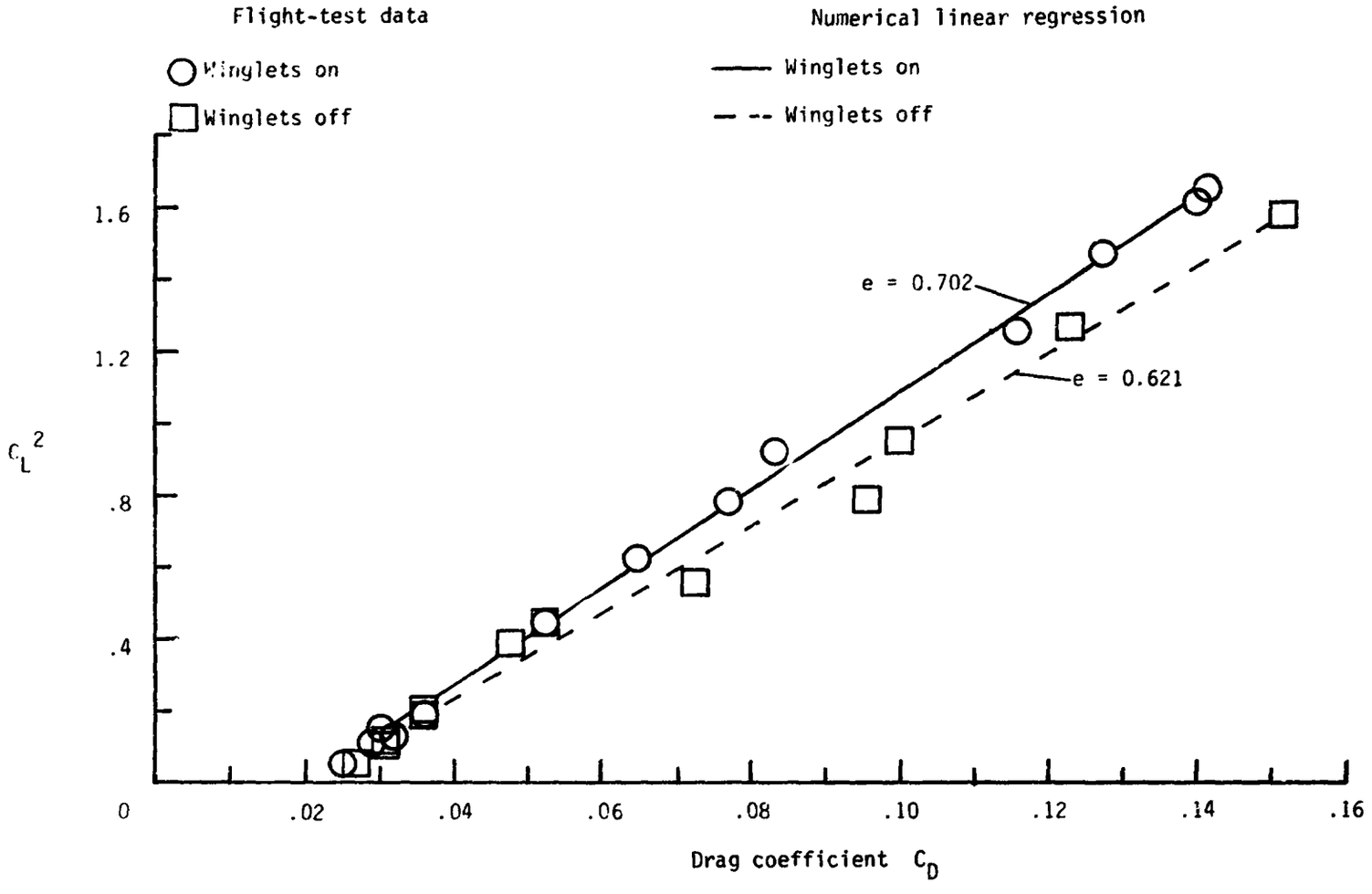


Figure 7.- Effect of winglets on airplane efficiency factor.

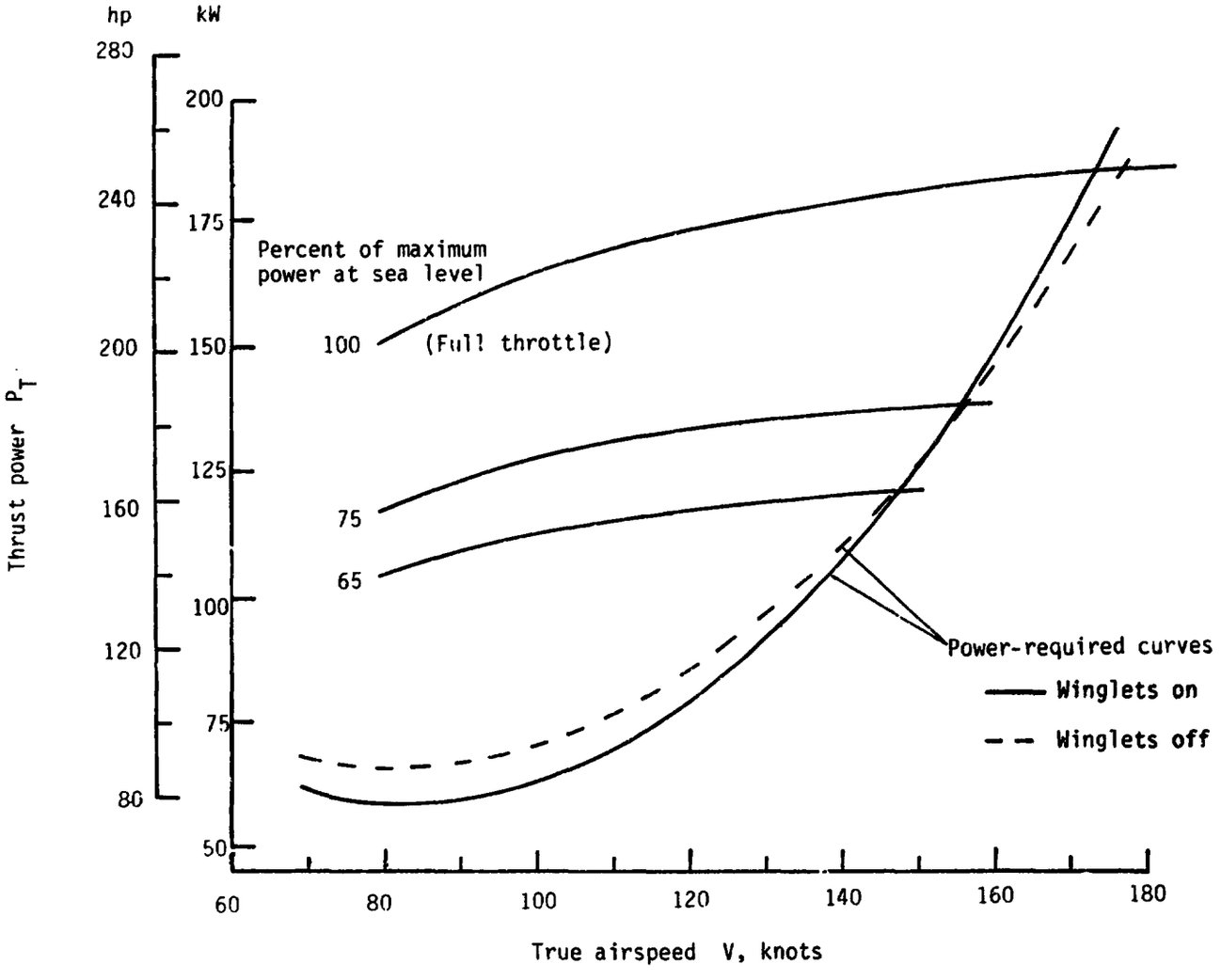


Figure 8.- Influence of winglets on speed-power performance at sea level. Power-required curves from numerically faired drag polars of figure 6. W = 16 014 N (3600 lb).

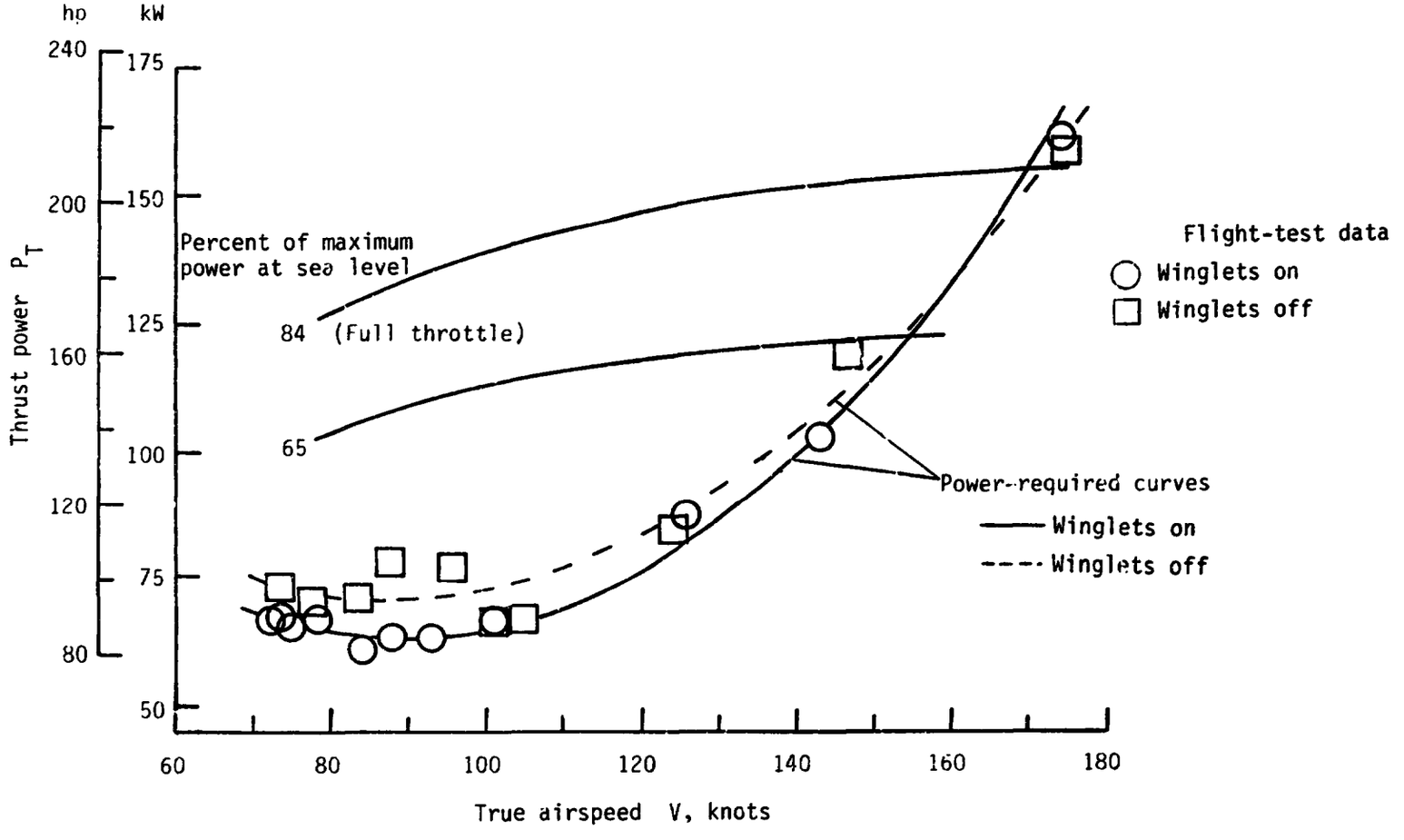


Figure 9.- Effect of winglets on speed-power performance at 1524 m (5000 ft) density altitude. Power-required curves from numerically faired drag polars in figure 6. W = 16 014 N (3600 lb).

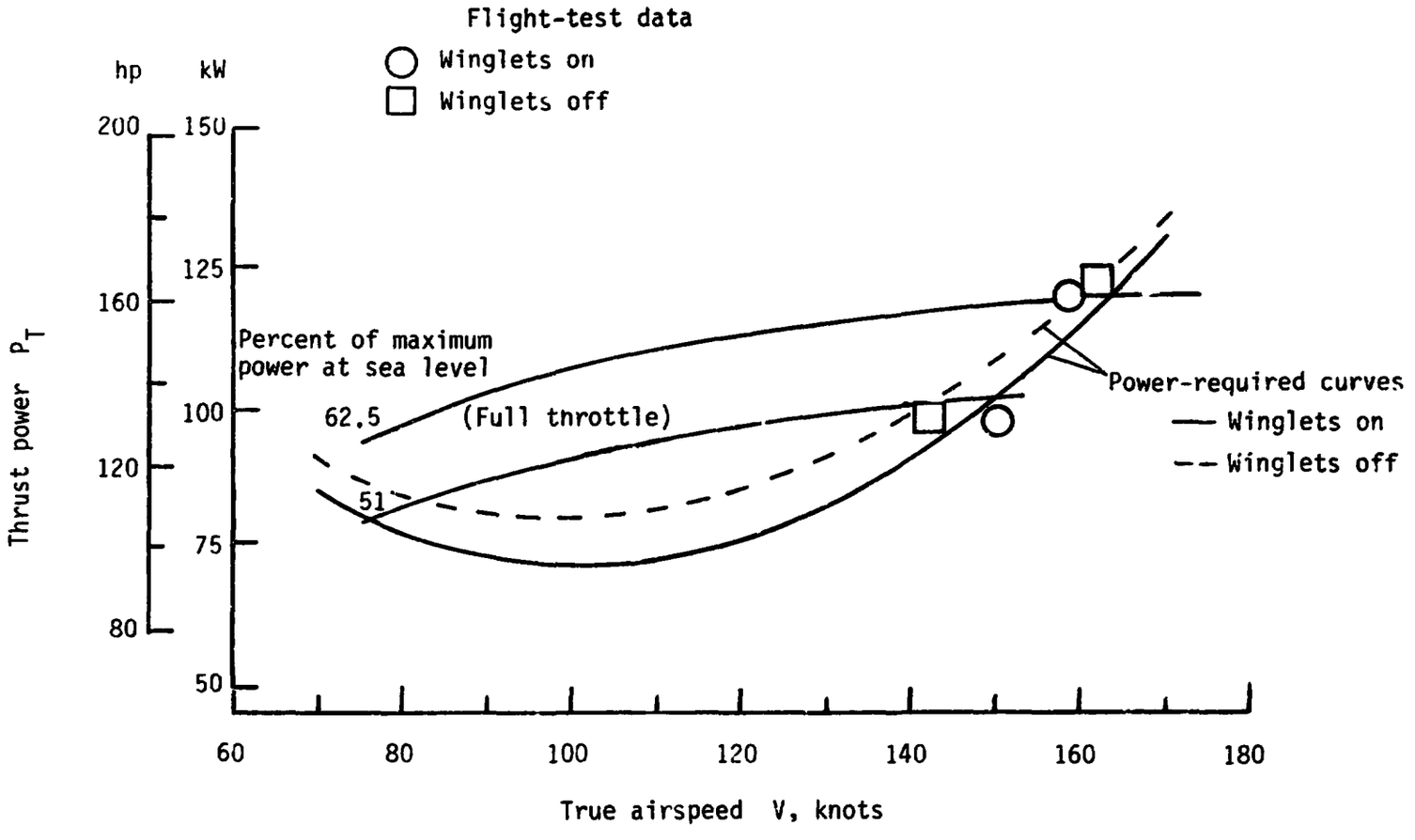


Figure 10.- Influence of winglets on speed-power performance at 3962 m (13 000 ft) density altitude. Power-required curves from numerically faired drag polars in figure 6. W = 16 014 N (3600 lb).

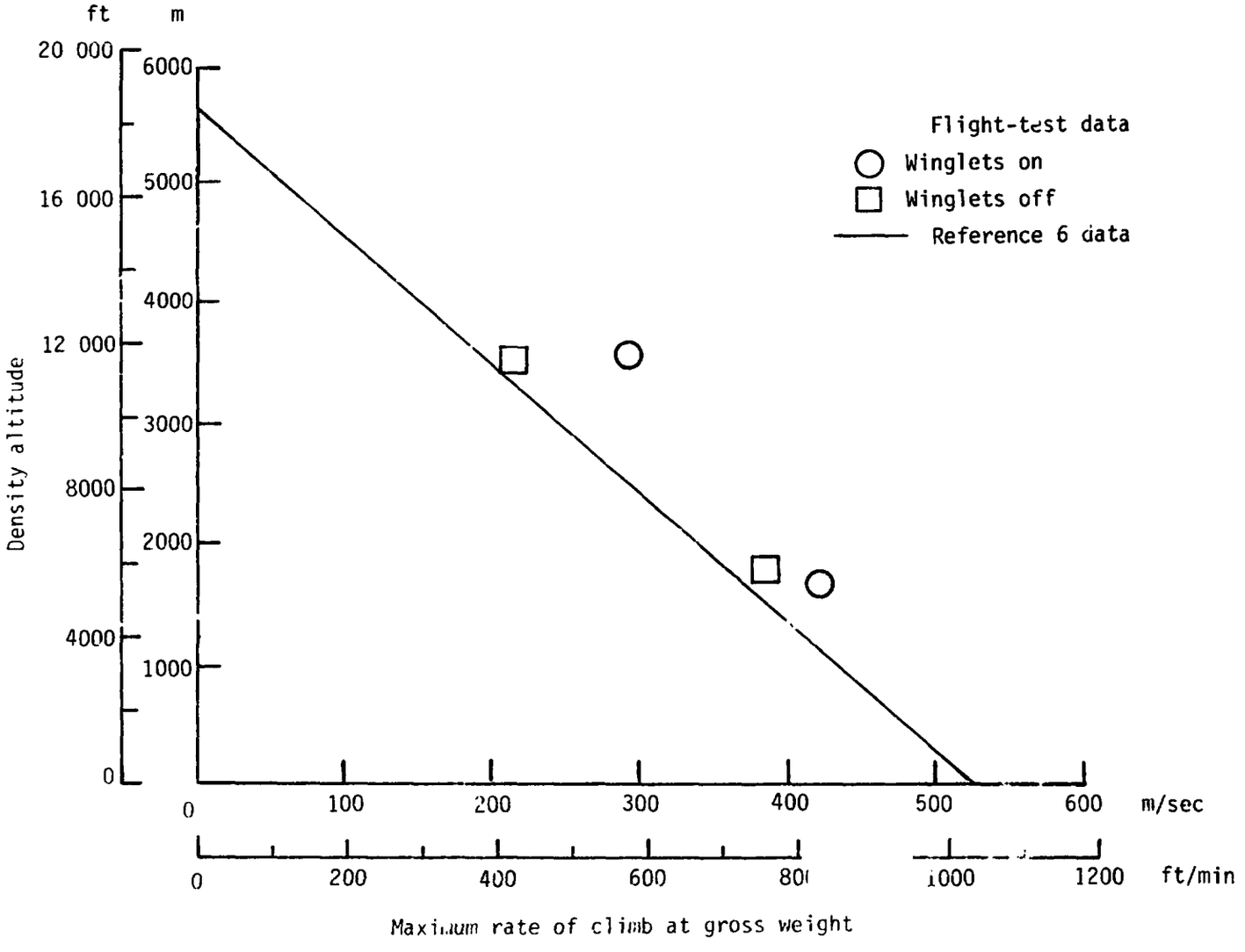


Figure 11.- Effect of winglets on maximum rate of climb.

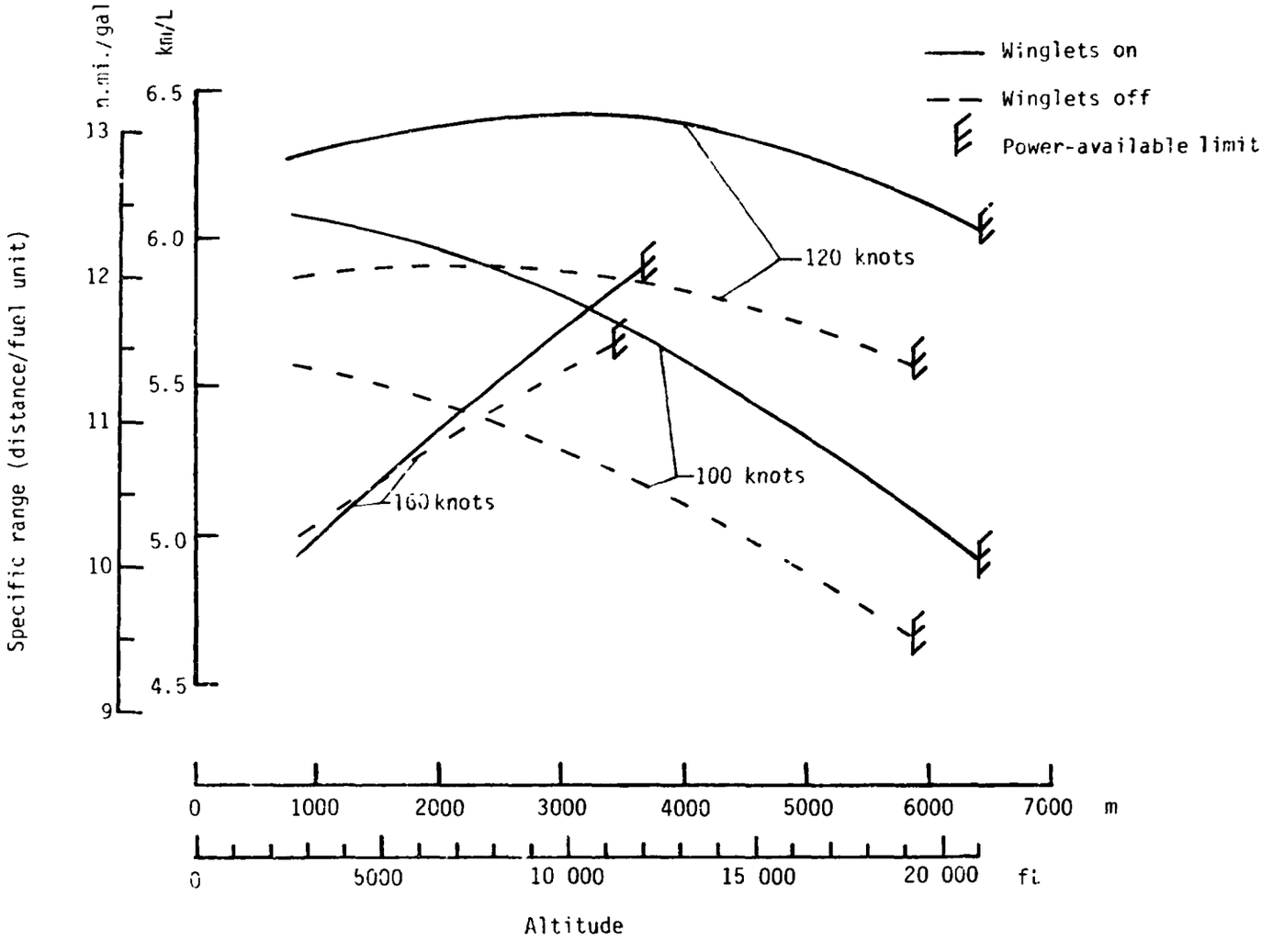


Figure 12.- Influence of winglets on airplane specific range. Curves obtained from numerically faired drag polars (fig. 6) and fuel-consumption data of reference 6. W = 16 014 N (3600 lb), $\eta_p$ = 0.85.